Supplemental material

Hoefert et al., https://doi.org/10.1083/jcb.201708173

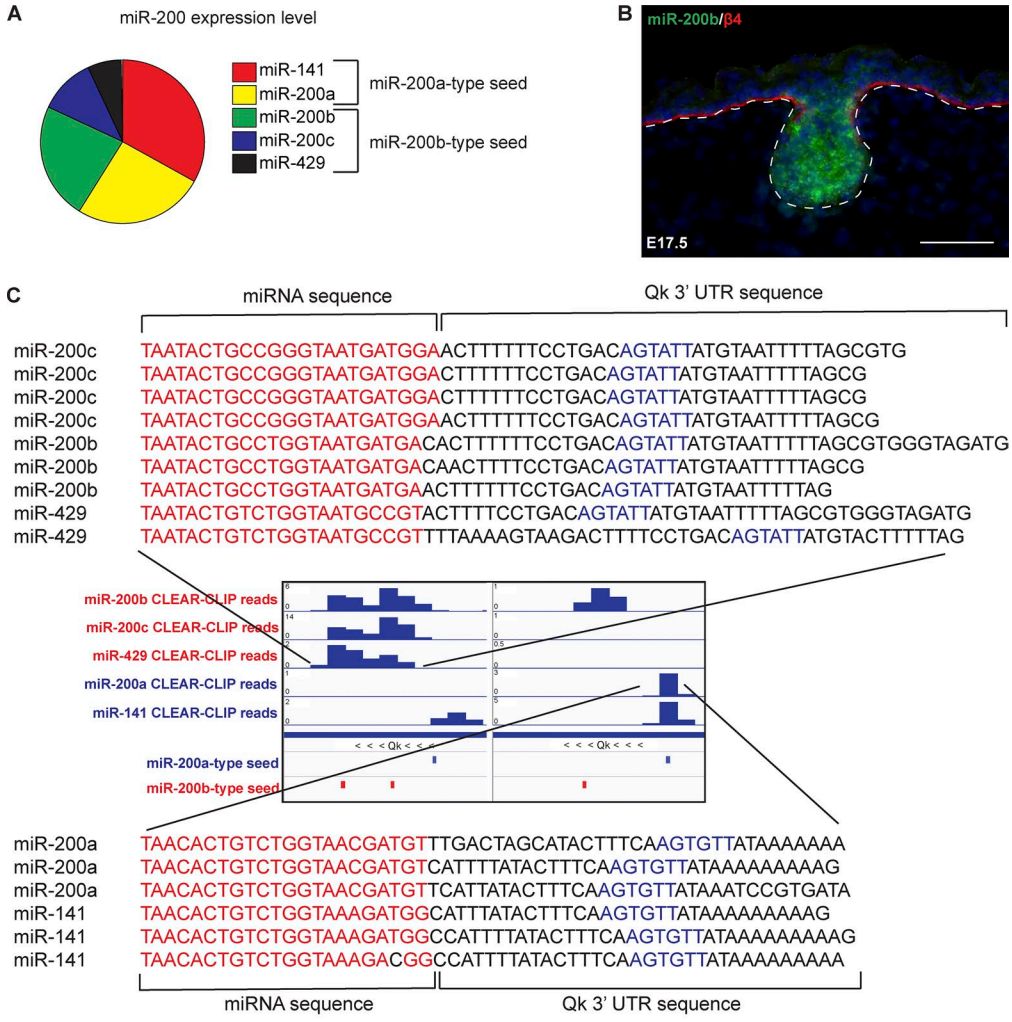

D

KEGG pathways enriched in CLEAR-CLIP	FDR (q-value)
Pathways in cancer	5.35^{-23}
Endocytosis	4.32^{-17}
Focal adhesion	4.23^{-15}
Neurotrophin signaling pathway	6.95^{-15}
ErbB signaling pathway	2.18^{-14}
Renal cell carcinoma	6.57^{-13}
Chronic myeloid leukemia	1.25^{-12}
Ubiquitin-mediated proteolysis	2.28^{-11}
MAPK signaling pathway	2.28^{-11}
Regulation of actin cytoskeleton	2.28^{-11}

GO Biological Process enriched in CLEAR-CLIP	FDR (q-value)
Tissue development	2.05^{-60}
Regulation of multicellular organism development	3.53^{-56}
Regulation of protein modification process	8.55^{-53}
Regulation of phosphorus metabolic process	7.02^{-52}
Regulation of transcription from RNA-pol II	7.07^{-52}
Phosphate-containing compound metabolic process	7.49^{-52}
Regulation of molecular function	8.71^{-52}
Regulation of intracellular signal transduction	1.52^{-51}
Cell development	4.28^{-49}
Positive regulation of protein metabolic process	6.94^{-49}

Figure S1. **miR-200 family expression pattern, representative CLEAR-CLIP reads, and target enrichment. (A)** Proportion of miR-200 family reads from each family member in miRNA-seq from Fig. 1 A. **(B)** In situ hybridization with a probe against miR-200b at E17.5. Bar, 50 µm. **(C)** Sequences of individual reads recovered from regions of the Qk 3′ UTR. miRNA sequence is shown in red, and seed sequence shown in blue. **(D)** GO-terms enriched within miR-200 targets identified with CLEAR-CLIP. Analysis was performed with the Molecular Signatures Database (MSigDb; Broad Institute). FDR, false discovery rate.

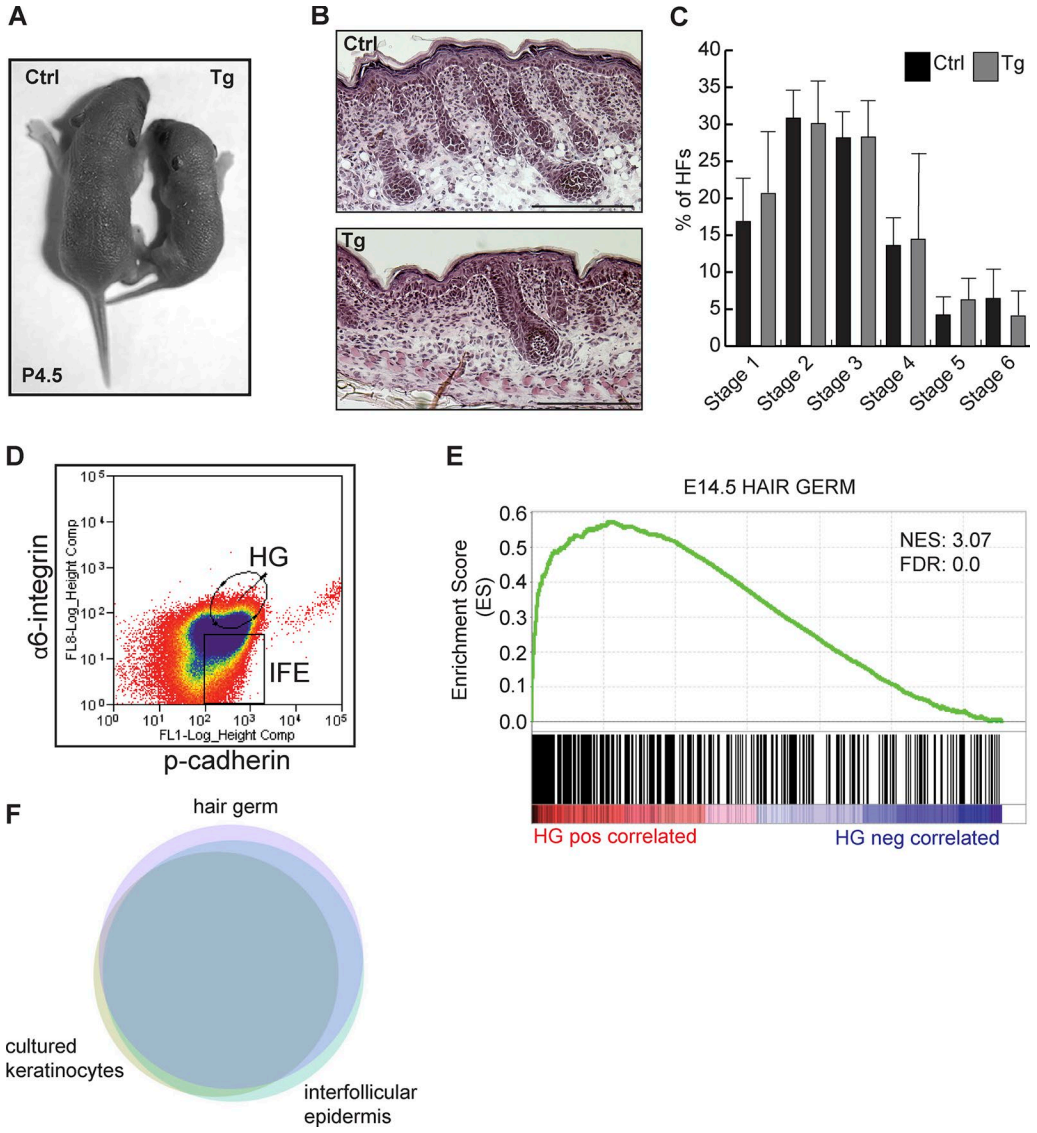

Figure S2. **Effect of miR-200 family expression on body size and hair follicles and validation of HG sorting. (A)** Control and Tg littermates at P4.5. **(B)** H&E staining on back skin from control and Tg animals at P0.5. Bars, 100 µm. **(C)** Percentage of hair follicles (HFs) at each stage of development in control and Tg animals at P0.5. *n* = 3. Error bars represent SD. **(D)** Sorting strategy used to isolate HG and IFE populations. **(E)** GSEA comparing HG population with a previously published E14.5 HG microarray signature (Rhee et al., 2006). FDR, false discovery rate; NES, normalized enrichment score. **(F)** Venn diagram comparing transcriptomes from cultured keratinocytes, HGs, and IFE.

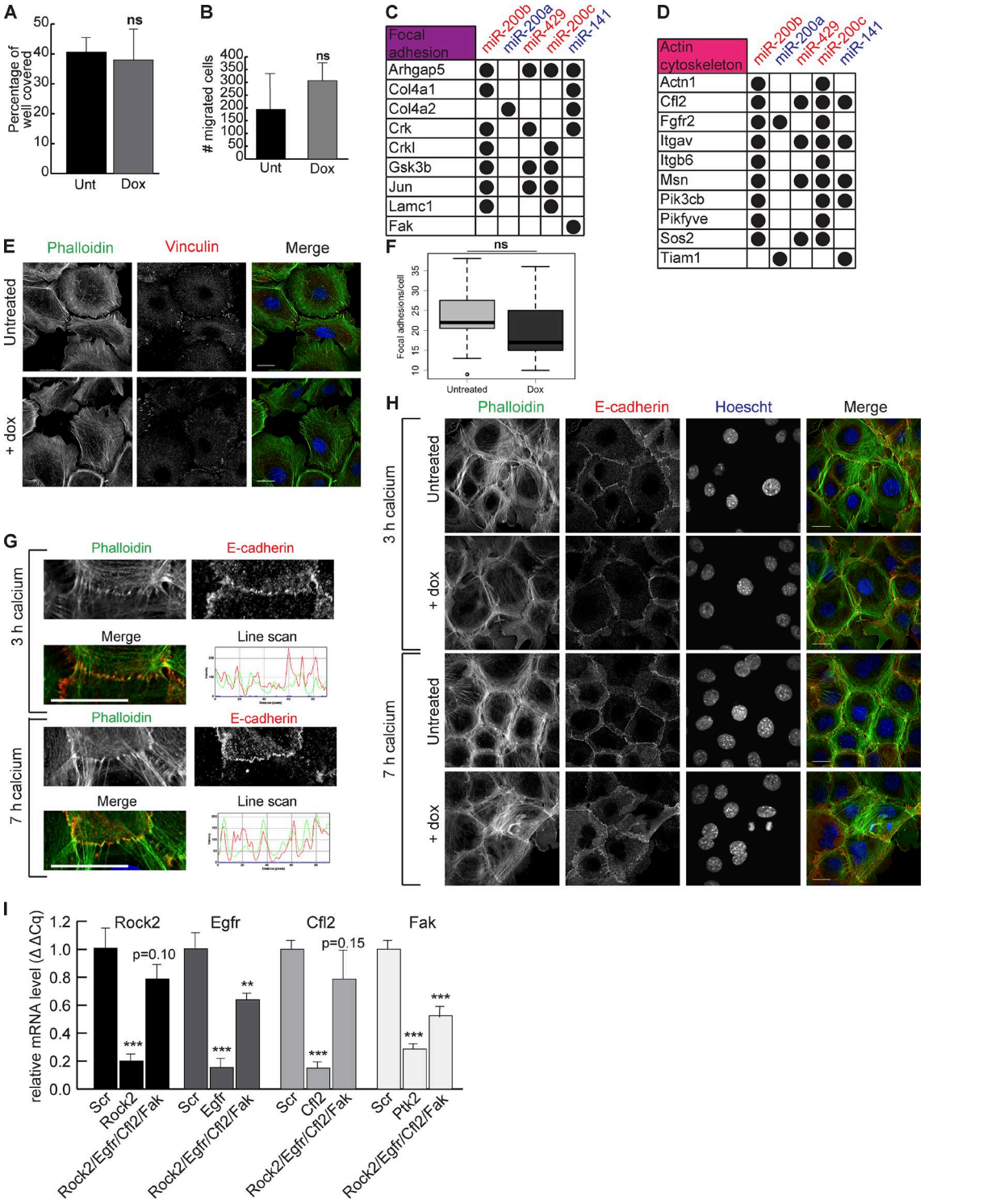

Figure S3. **miR-200s regulate proliferation, migration, FA, and cell junction formation. (A)** Percentage of wells covered by colonies formed by WT keratinocytes untreated (Unt) or treated with doxycycline (Dox). *n* = 3. **(B)** Number of cells migrated after 8 h in a scratch assay performed on WT keratinocytes untreated or treated with doxycycline. *n* = 3. **(C)** Extended list of miR-200 family targets identified with CLEAR-CLIP and RNA-seq involved in FA. **(D)** Extended list of miR-200 family targets identified with CLEAR-CLIP and RNA-seq involved in actin cytoskeleton. **(E)** Immunofluorescence of vinculin (red) and Phalloidin stain for actin (green) on WT keratinocytes untreated or treated with doxycycline. **(F)** Number of FAs per cell in E. *n* = 20 untreated and *n* = 20 doxycycline-treated cells. **(G)** Immunofluorescence of E-cadherin (red) and phalloidin staining for actin (green) on WT keratinocytes untreated or treated with doxycycline. Cells were treated with calcium for 3 or 7 h. RGB line scans were performed on 90 pixels across the length of each cell junction. Representative image from *n* > 20 junctions imaged for each condition. **(H)** Immunofluorescence of E-cadherin (red) and phalloidin staining for actin (green) on inducible keratinocytes untreated or treated with doxycycline and induced with calcium for 3 or 7 h. Representative images from *n* > 20 cell junctions imaged for each treatment. Full-sized images of selections are shown in Fig. 4 I. Bars, 20 µm. **(I)** Quantitative RT-PCR on WT keratinocytes infected with shRNAs. *n* = 3. **, P < 0.01; ***, P < 0.001; error bars show SD.

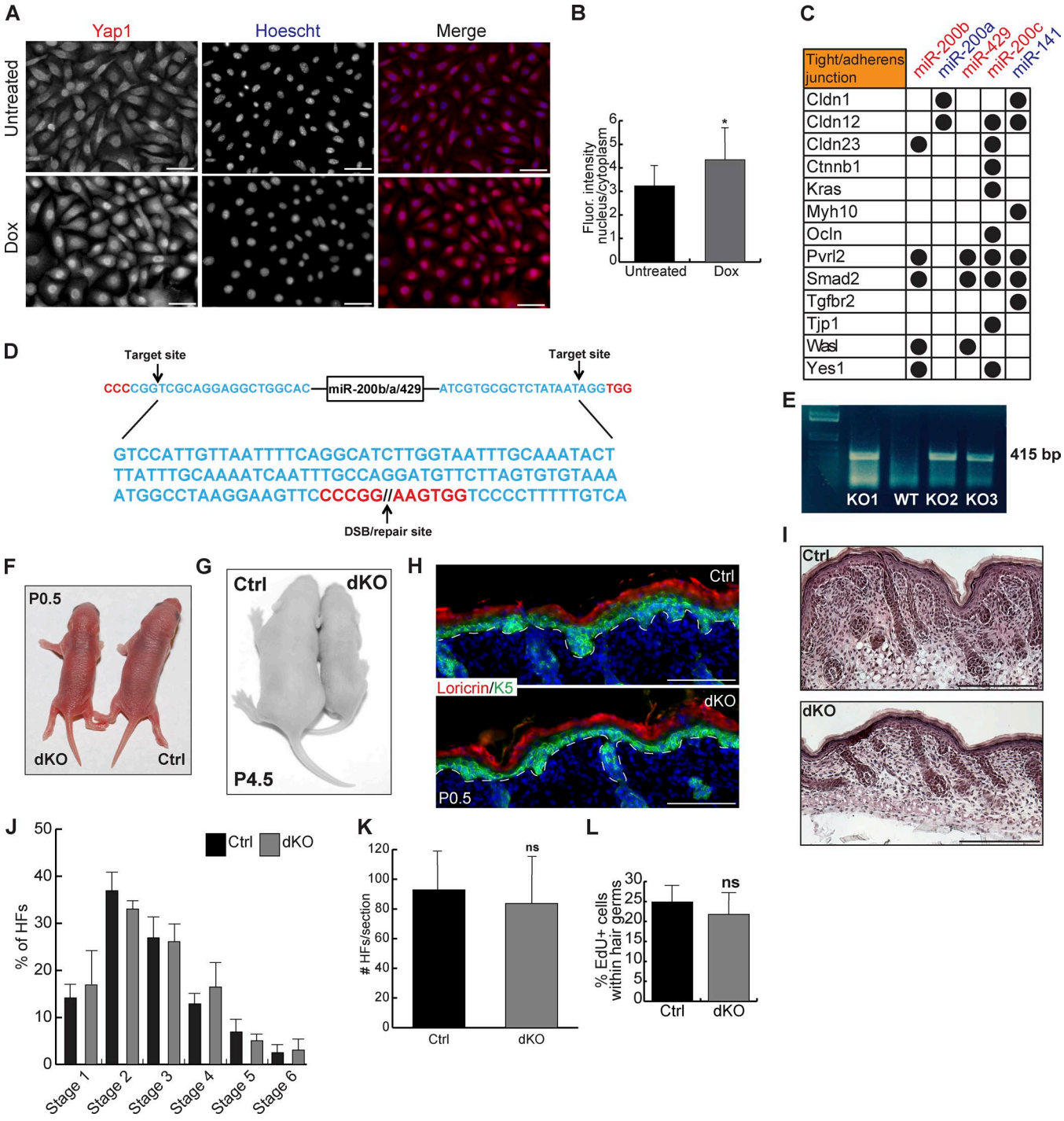

Figure S4. **Generation of a mouse model lacking miR-200s and the effect of the loss on body size and hair follicles. (A)** Immunofluorescence of Yap1 on inducible keratinocytes untreated or treated with doxycycline (Dox). **(B)** Fluorescence intensity of nucleus compared with cytoplasm from cells in A. $n = 3$. **(C)** Extended list of miR-200 family targets identified with CLEAR-CLIP and RNA-seq involved in tight junctions and AJs. **(D)** Sequencing result from one of the miR-200b cluster KO founder mice generated through CRISPR. Top arrows indicate expected cut sites, and the bottom arrow shows the repaired sequence. DSB, double-strand break. **(E)** Genotyping band showing null allele in a miR-200b KO mouse. **(F)** Control and miR-200 dKO littermates at P0.5. **(G)** Control and miR-200 dKO littermates at P4.5. **(H)** Immunofluorescence for loricrin (red) and keratin-5 (green) in back skin of control and dKO animals at P0.5. Representative images from $n = 3$ pairs of animals. **(I)** H&E staining on back skin from control and dKO animals at P0.5. Bars: (A) 50 µm; (H and I) 100 µm. **(J)** Percentage of hair follicles (HFs) at each stage of development in control and Tg animals at P0.5. $n = 3$. **(K)** Number of hair follicles per section in control and dKO back skin at P0.5. $n = 3$. **(L)** Percentage of EdU$^+$ cells in HGs of control and dKO animals at P0.5. $n = 4$. Error bars represent SD.

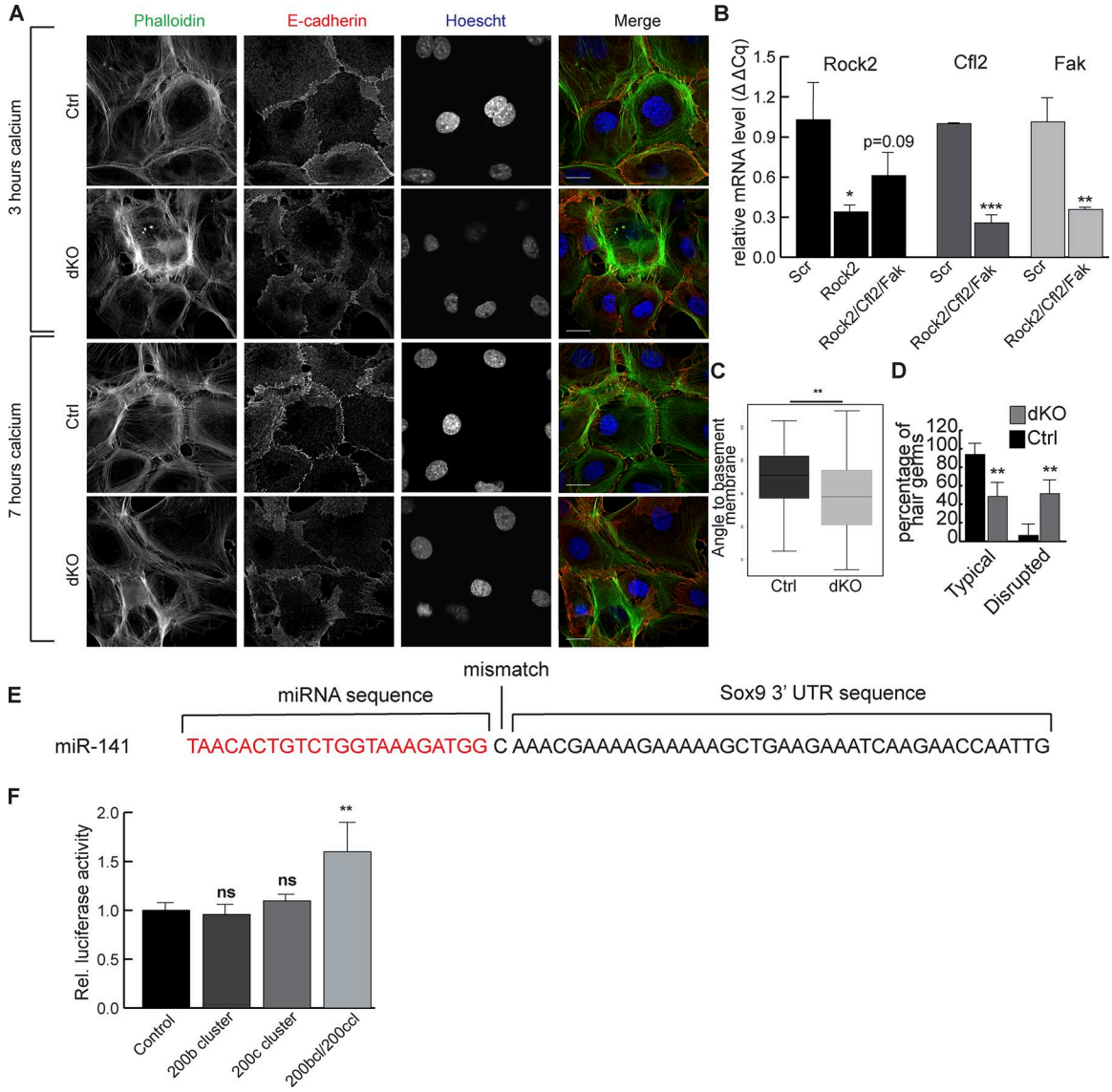

Figure S5. **Loss of miR-200s affects cell junction formation and cell orientation, and miR-200s do not directly regulate Sox9. (A)** Immunofluorescence of E-cadherin (red) and phalloidin staining for actin (green) on control and dKO keratinocytes induced with calcium for 3 or 7 h. Representative images from $n > 20$ cell junctions imaged for each treatment. Full-sized images of selections are shown in Fig. 8 N. Bars, 20 µm. **(B)** Quantitative RT-PCR on dKO keratinocytes infected with shRNAs. $n = 3$. **(C)** Angle of HG cells relative to the basement membrane from control and dKO animals at P0.5. $n = 4$ pairs of animals, $n = 16$ control cells, and $n = 30$ dKO cells. **(D)** Percentage of HGs from control and dKO animals at P0.5 with typical or disrupted cell polarity as imaged with pericentrin in Fig. 10 E. $n = 4$. **(E)** A CLEAR-CLIP read for miR-141 ligated to the 3′ UTR of Sox9. **(F)** Relative luciferase activity of Sox9 3′ UTR with the addition of the miR-200b cluster, the miR-200c cluster, or both. $n = 6$. *, $P < 0.05$; **, $P < 0.01$; ***, $P < 0.001$; error bars represent SD.

Table S1. **Primers used in this study**

Oligonucleotide	Sequence (5′–3′)
CRISPR; L gRNA for miR-200b cluster	GTGCCAGCCTCCTGCGACCG
CRISPR; R gRNA for miR-200b cluster	ATCGTGCGCTCTATAATAGG
cloning; 200b luciferase reporter; forward	CTAGATCATCATTACCAGGCAGTATTAGATCTCATCATTACCAGGCAGTATTAC
cloning; 200b luciferase reporter; reverse	TCGAGTAATACTGCCTGGTAATGATGAGATCTAATACTGCCTGGTAATGATGAT
cloning; 141 luciferase reporter; forward	CTAGACCATCTTTACCAGACAGTGTTAGATCCCATCTTTACCAGACAGTGTTAC
cloning; 141 luciferase reporter; reverse	TCGAGTAACACTGTCTGGTAAAGATGGGATCTAACACTGTCTGGTAAAGATGGT
cloning; 200c luciferase reporter; forward	CTAGATCCATCATTACCCGGCAGTATTAGATCTCCATCATTACCCGGCAGTATTAC
cloning; 200c luciferase reporter; reverse	TCGAGTAATACTGCCGGGTAATGATGGAGATCTAATACTGCCGGGTAATGATGGAT
cloning; miR-200b cluster; forward	GTTGACCTCTCCACTACCTA
cloning; miR-200b cluster; reverse	ACCAGTGTTGATAGCACAGG
cloning; cyclin G2 3′ UTR; forward	CACAGACTGGAATACCTACCTTC
cloning; cyclin G2 3′ UTR; reverse	GCACTGACCAATTATCACACA
cloning; Ptpn14 3′ UTR; forward	GTCCCTCAGTACCAGAAGAAATG
cloning; Ptpn14 3′ UTR; reverse	GAGGGAACAGTGCAAAGGAATA
cloning; Ywhab 3′ UTR; reverse	GCTCAGACTGGTCCCTTAATAC
cloning; Ywhab 3′ UTR; reverse	CCACCACAGAAGCAAACATTAG
cloning; Snai2 3′ UTR; forward	TGGCGCAACCAGTGTTTA
cloning; Snai2 3′ UTR; reverse	GTGGCTATTAACCGTACCTCAC
cloning; Cfl2 3′ UTR; forward	CCCGTTCGTGAATGAGTGAATA
cloning; Cfl2 3′ UTR; reverse	TGTGAGGGTAGGGAGTTTGA
cloning; Ccnd2 3′ UTR; forward	CGTTTGGTTCCGTTTGGTTC
cloning; Ccnd2 3′ UTR; reverse	GTCTTAGCCTGTTGCTCCTATAA
cloning; Lats1 3′ UTR; reverse	TATGAACTGAGTATTATAGTCAAT
cloning; Lats1 3′ UTR; reverse	TGAACAAAATACTAAAATTGCAGA
cloning; Lats2 3′ UTR; reverse	TGCATTAAAACAGTATTTTTAAAA
cloning; Lats2 3′ UTR; reverse	TAGCGAGAATACTGTAAGTCACAA
cloning; Fat1 3′ UTR; reverse	CCATTTCCAGCGTCCTAACT
cloning; Fat1 3′ UTR; reverse	CCTTTACAAGACCATTGCATCAC
cloning; Fat2 3′ UTR; reverse	GGGTGAGAACTAGGAGGGTAAT
cloning; Fat2 3′ UTR; reverse	CCAAAGCCACTTGTGCAATC
genotyping; pTRE2-200bcl; forward	ATGCTGCCCAGTAAGATGGC
genotyping; pTRE2-200bcl; reverse	CCTACAGCTCCTGGGCAACGTG
genotyping; K14 forward primer for K14rtTA and K14cre	TGGGCGGGTGCCGAGAT
genotyping; K14rtTA; reverse	TGCTGTTTCACTGGTTATGCGG
genotyping; cre; reverse	TTGCCCCTGTTTCACTATCCAG
genotyping; miR-200c cluster floxed allele; forward	CAACAGCCTCTGACCTTTAACC
genotyping; miR-200c cluster floxed allele; reverse	CCTTCTGGGCAGACAAGAATAC
genotyping; miR-200bcl CRISPR KO, left side; forward; forward for KO band	GCTGAGCATCCGGAAAAGTA
genotyping; miR-200bcl CRISPR KO, left side; reverse	CAGGCTACCTCTTAGTGGCTGT
genotyping; miR-200bcl CRISPR KO, right side; forward	ATGGGGAGTTTGAGTGTTGC
genotyping; miR-200bcl CRISPR KO, right side; reverse; reverse for KO band	TGCAAGGCTGCTTGTTAATG
qPCR; Cyr61; forward	CCCCCGGCTGGTGAAAGT
qPCR; Cyr61; reverse	GCGGTTCGGTGCCAAAGA

Table S1. **Primers used in this study *(Continued)***

Oligonucleotide	Sequence (5′–3′)
qPCR; Ctgf; forward	GGGCCTCTTCTGCGATTTC
qPCR; Ctgf; reverse	ATCCAGGCAAGTGCATTGGTA
qPCR; Lats2; forward	GGACCCCAGGAATGAGCAG
qPCR; Lats2; reverse	CCCTCGTAGTTTGCACCACC
qPCR; Cfl2; forward	GCATCTGGAGTTACAGTGAATGA
qPCR; Cfl2; reverse	CACCAATGTCACCCACCAAGA
qPCR; Cyclin E2; forward	ATGTAAGACGCAGCCGTTTA
qPCR; Cyclin E2; reverse	GCTGATTCCTCCAGACAGTACA
qPCR; Celsr1; forward	TCGCTGACTTCGGTGCTTG
qPCR; Celsr1; reverse	TTACCAGCTCTACCCAAACGG
qPCR; Met; forward	GTGAACATGAAGTATCAGCTCCC
qPCR; Met; reverse	TGTAGTTTGTGGCTCCGAGAT
qPCR; Egfr; forward	GCCATCTGGGCCAAAGATACC
qPCR; Egfr; reverse	GTCTTCGCATGAATAGGCCAAT
qPCR; Ptk2/Fak; forward	TTAGGCGATCCTATTGGGAGATG
qPCR; Ptk2/Fak; reverse	TTCTTAGTGTTTTGGCCTTGACA
qPCR; Rock2; forward	TTGGTTCGTCATAAGGCATCAC
qPCR; Rock2; reverse	TGTTGGCAAAGGCCATAATATCT
CLEAR-CLIP; 3′ linker	NNTGGAATTCTCGGGTGCCAAGG
CLEAR-CLIP; 5′ Linker	GUUCAGAGUUCUACAGUCCGACGAUCNNNN
CLEAR-CLIP; RT primer	GCCTGGCACCCGAGAATTCCA
CLEAR-CLIP; library first round F primer	GTTCTACAGTCCGACGAT

Reference

Rhee, H., L. Polak, and E. Fuchs. 2006. Lhx2 maintains stem cell character in hair follicles. *Science.* 312:1946–1949. https://doi.org/10.1126/science.1128004